

Bio-based composite as phase change material including spent coffee grounds and beeswax paraffin

Moez Souissi*, Abdelwaheb Trigui**,†, Ilyes Jedidi****, Mohamed Sahbi Loukil****, Makki Abdelmouleh*,†

*Laboratoire de Sciences des Matériaux et de l'Environnement (LMSE), Université de Sfax, Tunisia

**Laboratoire des Matériaux Multifonctionnels et Applications (LaMMA), Université de Sfax, Tunisia

***University of Technology and Applied Sciences - Sohar, P.O. Box: 135, Postal Code:311, Sohar, Sultanate of Oman

****Division of Engineering Materials (KMAT), Linköping University, 581 83, Sweden

(Received 5 October 2022 • Revised 25 December 2022 • Accepted 31 January 2023)

Abstract—New types of bio-composite phase change materials (BCPCM) with improved thermal properties were made from spent ground coffee powder (C), beeswax (W) and low density polyethylene (LDPE). Beeswax is a relatively accessible phase change material of organic origin, with a significantly lower unit price compared to conventional phase change materials (PCM). The observations by SEM and FTIR spectroscopy showed that the BCPCMs were physically combined. Through these techniques, it was discovered that ground coffee was effectively impregnated with natural wax and LDPE. According to the thermal gravimetric analysis (TGA), the thermal stability of BCPCM was improved, due to the use of waste coffee grounds, in the working temperature range. The biocomposite possesses excellent performance as characterized by 136.9 J/g (W70C10PE20)>, 127.31 J/g (W70C20PE10)>, 126.95 J/g (W70C30)>, 121.08 J/g (W70PE30) of latent heat storage and tends to decrease the supercooling degree as compared with pure beeswax during melting/solidification process. By adding LDPE to the PCM, the melting time is reduced, demonstrating an improvement in thermal energy storage (TES) reaction time to the demand. The experimental results showed that the fraction of oils (12%) in spent ground coffee powder can participate in the improvement of the thermal properties of BCPCM. The use of biocompatible PCM by-products is suitable for applications in the field of heat storage because it is affordable and environmentally beneficial.

Keywords: Bio-composite, Phase Change Material (PCM), Spent Coffee Ground, Beeswax, Low Density Polyethylene (LDPE)

INTRODUCTION

Global warming and the scarcity of fossil energy sources have led to the search for new solutions that consume less energy, which are cleaner than current methods. Latent thermal storage is one of the options being examined to reduce consumption. The use of phase change materials (PCMs) makes it possible to store and release large amounts of heat with reduced volumes by using latent heat storage during melting and solidification at specific temperatures. Indeed, through solid-liquid phase shift, PCMs reduce temperature variations and improve solar energy consumption [1-5]. Over the past ten years, research on PCMs has gradually increased, and comprehensive evaluations of PCMs and their applications are available [6-8]. Therefore, one of the key intended goals is the development of phase change materials (PCM) with high energy storage density and recyclable solid-liquid phase behavior [9,10]. Latent heat storage biocomposites (LHSBCs) by natural wax have received considerable attention due to their controllable phase change temperature, stable physical and chemical properties, and high biological safety (e.g non-toxic, non-odorous, and non-irritant) [11].

Beeswax is mainly composed of a mixture of esters of hexadeca-

noic and octadecanoic acids, with fatty alcohols having chain lengths between 38-52 and 46-54 carbon atoms, respectively [12]. These molecular structural characteristics, which lead to a relatively high enthalpy of fusion, make beeswax an attractive candidate for energy storage as PCM [13]. However, the applications of natural waxes are limited by leakage during the energy storage process. Meanwhile, low thermal conductivity also compresses the conduction and conversion of solar thermal energy [14,15]. Mixing waxes with useful polymers is one way to preserve them in a stable state during application. Wax leakage is eliminated, and the wax is fixed in a compact condition even after melting thanks to the polymer matrix. Polymer composites are easily shaped materials, and the polymer phase brings its own specific properties. Polyethylene seems to be the most frequently used polymer to be mixed with paraffin waxes to obtain shape stabilized PCM [16-18]. For example, Inaba and Tu [17] have investigated a form-stabilized paraffin wax system based on paraffin wax mixed with high-density polyethylene (HDPE). Nevertheless, Krupa et al. [19] have studied the thermal and thermomechanical properties of stabilized phase change materials based on low-density polyethylene and Fischer-Tropsch paraffin waxes. The amount of LDPE at such a high wax level was found to be inadequate to keep the structure of the material in a consistent shape, even if LDPE still forms the continuous phase up to 50% wax.

The production of shape-stable beeswax materials is crucial for

†To whom correspondence should be addressed.

E-mail: abdotrg@yahoo.fr, makki.abdmouleh@yahoo.fr

Copyright by The Korean Institute of Chemical Engineers.

resolving these issues [15,20]. One strategy is the preparation of porous CPCMs via biomass or biomass waste, as it not only reduces the cost of preparing solar thermal energy storage materials, but also accelerates the energy revolution and reduces the pollution caused by both the consumption of fossils and the dumping of biomass [4,21]. Coffee is the second most important commercial product that creates a large amount of spent coffee grounds (SCG) every year [22]. SCGs that are still underutilized have recently been applied to fabricate CPCMs [23,24]. Actually, some cases of effective use of SCGs have much inspired us.

Currently, spent coffee grounds (SCG) are attracting more attention due to the significant amount of wasted coffee grounds (SCG) produced daily (food waste from coffee processing) [25]. SCG are currently gaining much interest as a natural filler for polymer matrices such as poly(lactic acid) (PLA) [26] and polypropylene [25]. Among the organic materials that make up these particles are celluloses, hemicelluloses, lignins and fatty acids [26,27]. These compounds are known to impart high stiffness and flexibility to biocomposites [28]. SCG has also been used thanks to its high content of polysaccharides, phenolics and protein compounds, as well as the production of several important compounds like ethanol, biodiesel and mannitol [29]. Besides, it is an effective substance for vegetable compost by providing cellulose, ash, calcium and phosphorus after they decompose in the soil [28]. Like other bio-fillers, however, SCGs have poor water resistance because of their high hydrophilicity, which limits compatibility with most polymers (hydrophobic) [26], leading to a poor filler/matrix (voids) interface, therefore poor mechanical performance of biocomposites [30,31]; limiting large-scale uses [32].

SCGs could be combined with other biomasses like natural waxes to make PCM bio-composites [33]. It could also be applied to synthesize activated carbon (AC), SCGs-AC showed high impregnation rate of SCG-based CPCMs and high latent heat capacity [34]. Other works [35] have shown that the introduction of (reduced graphene oxide) RGO into CPCMs can effectively improve the adsorption of SCG on polyethylene glycol (PEG) and at the same time improve the thermal conductivity and the light absorption performance of CPCMs in the entire UV-Vis-NIR range. Therefore, it remains difficult to improve the thermal conductivity and the adsorption rate of SCGs for PCMs at low cost. SCGs-AC demonstrated a high impregnation rate of SCG-based CPCMs and a high latent heat capacity, and it could also be used to synthesize activated carbon (AC) [33].

Shape-stabilized PCMs (ss-PCMs) are generally synthesized by blending PCMs with supporting materials. However, most of those PCMs are fabricated via complex procedures with corrosive or toxic chemicals, leading to high cost and environmental concerns. Biopolymers have also been used as the supporting materials. SCG is a renewable, abundant in nature with distinct advantages, such as low cost, good biocompatibility, non-toxicity, environmental friendliness [36]. Without crosslinking, SCG can be quickly and environmentally friendly converted into a three dimensional (3D) hierarchical porous scaffold without crosslinking [37,38]. It is suitable for multiple applications, namely drug delivery [39], supercapacitors [38], wastewater treatment [40], thermal insulators [41], organic catalysts [42].

However, up to now, the study reports about utilizing beeswax as the supporter of shape-stabilized phase change materials are still rare. As a result, ongoing efforts are needed to study the immobilization of organic phase change materials in the addition of SCG.

In the search for efficient and sustainable PCMs, the present research work describes three approaches pertaining to the production of bio-CPCMs based on renewable feedstocks. The idea is to develop BCPCMs based on beeswax/LDPE and to test the thermal storage capacity and stability after the integration of SCG micro-fillers in the composite.

EXPERIMENTAL SECTION

1. Materials

Spent coffee grounds (C) were collected after brewing roasted coffee beans (Boundin, Tunisia) in an automatic coffee machine. A specific treatment was carried out on these coffee beans to obtain (C) microparticles (Schema 1). After being cleaned with water, used coffee grounds were dried in an oven for 24 hours at 100 °C. Subsequently, 10 g of powder were introduced into an agate flask with beads 6 mm in diameter. The flask was then sealed and placed in a Retsch planetary Ball Mill where the powder was ground (400 rpm) for 1 h at room temperature.

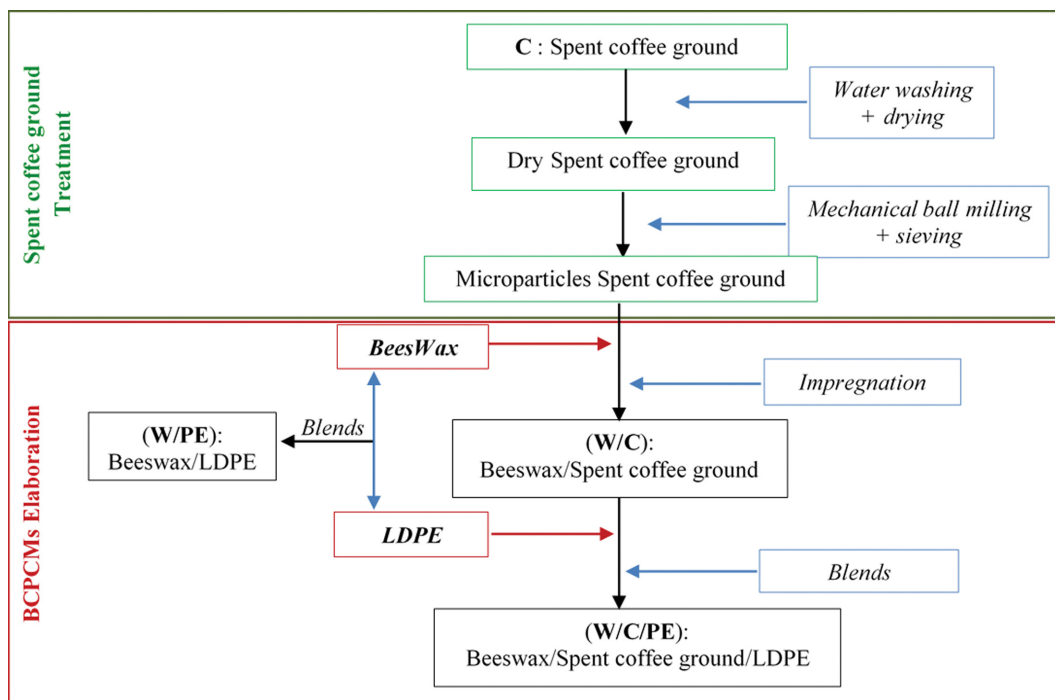
The selected PCM used in this work was beeswax. The beeswax had a density of 0.773 g/cm³ and a phase change temperature of roughly 60 °C. The low-density polyethylene (LDPE) in pellets used in this work has a melting temperature of 107 °C and a density of 0.9 g/cm³.

2. Preparation of BCPCMs

The samples, presented in Table 1 (was used for abbreviation), were prepared using the melt-mix method (i) and the impregnation method (ii) (Schema 1). The beeswax in pellet form was melted at 60 °C for 60 min under magnetic stirring at 200 rpm. For the filled composites, the dry spent coffee grounds microparticles were gradually added to the liquid mixtures with stirring (impregnation phase). The LDPE was added and immediately mixed with the liquid phase wax. The mixture was agitated for two hours at a speed of roughly 1,200 rpm to ensure uniform dispersion of the PCM in the LDPE. Then, the temperature was set at 120 °C and LDPE was

Table 1. List of samples composition (Weight %)

	Beeswax (W)	LDPE (PE)	SCG (C)
W100	100	-	-
PE100	-	100	-
W90PE10	90	10	-
W80PE20	80	20	-
W70PE30	70	30	-
W60PE40	60	40	-
W50PE50	50	50	-
W80C20	80	-	20
W70C30	70	-	30
W60C40	60	-	40
W70C20PE10	70	10	20
W70C10PE20	70	20	10



Schema 1. Different steps of the process developed for the preparation of BCPCMs.

added to the Beeswax/LDPE mixture. The mixture was stirred at 2,000 rpm for three hours until it became a homogenous viscous liquid. After cooling to room temperature, the Beeswax/LDPE composites were finally obtained. The samples were then melt pressed at 120 °C into 100 mm×100 mm×2 mm sheets using a 10-ton AMS hot melt press. The various mass ratios of the constituent parts in each of the 50 g samples are displayed in Table 1.

3. Characterizations

Scanning electron microscopy (SEM): The microstructure of samples was represented by scanning electron microscopy (SEM) at room temperature. A SEM with an accelerating voltage of 12 kV and a working distance of 12 mm was used to collect the SEM images.

Fourier-transform infrared spectroscopy (FTIR): All composites were examined using a Perkin Elmer FTIR system spectrum BX employing an ATR mode between 4,000-500 cm^{-1} to identify the functional groups.

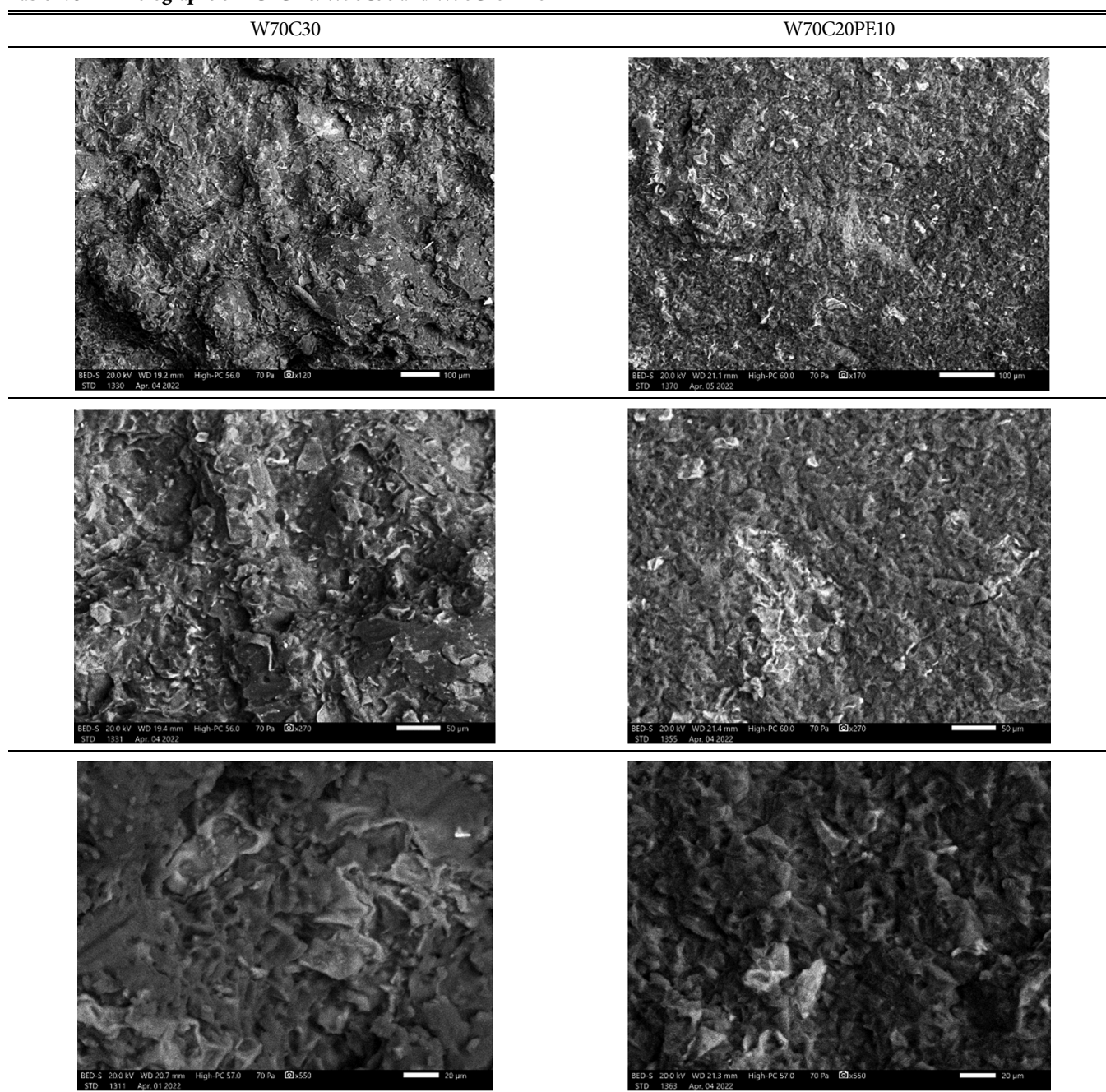
Thermogravimetric analysis (TGA): Thermogravimetric analysis (TGA) was realized on a Perkin-Elmer TGA7 analyzer. The heating rate was 10 °C/min and the sample weight was in the order of 4 mg. Thermograms were recorded over a temperature range of 30-800 °C carried out under an oxygen atmosphere with the flow rate of 20 ml/min.

Differential scanning calorimetry (DSC): The DSC calorimeter is a Perkin-Elmer DSC7 with 20 mL/min flow of N_2 . The signal is analysed without subtraction. A sample mass of 2-5 mg and heating rate of 10 °C/min were used.

IR thermography: The effectiveness of heat transfer for the various kinds of PCM composite samples utilized in this study was evaluated using an IR thermography test. FLIR C3 was used as the IR camera, with a cylindrical shape of 30 mm in diameter.

RESULTS AND DISCUSSION

To study the dispersion of spent ground coffee microparticles in PCM, the composites BCPCM prepared by impregnation and hot uniaxial compression are fractured at low temperature. The SEM observations of the fracture surfaces are shown in the photos in Table 2. The observations of the W70C30 bio-composite show that the beeswax is absorbed in the pores and on the surface of the coffee grounds particles thus ensuring a fairly dense material [43]. The porous structure of the coffee grounds particles ensures the mechanical strength of the composite assembly and can prevent the leakage of molten PCM [24,33,44]. For the composites in the presence of LDPE (W70C20PE10), the impregnation of the wax on the microparticles of the coffee grounds was well noted. A heterogeneous surface was observed by the presence of empty zones linked to a phase separation indicating the immiscibility of LDPE with beeswax [45]. Indeed, the low percentage of LDPE does not allow all of the low molecular weight wax chains to penetrate into the branching network of the LDPE chains. The amorphous structure of the polymer due to its low crystallinity [46] means less packing of the polymer chains become saturated with wax chains. Wax cohesion occurs due to high wax intermolecular attractive forces during melt processing. For a very high wax content (70%), even the open areas in the low density PE are not sufficient to accommodate the wax chains and the phenomenon of agglomeration can take place, thus favoring the immiscibility of the mixture. The spent ground coffee microparticles was found to a good structure for incorporating liquefied materials, such as PCMs. SEM analysis show that beeswax incorporated well into the structure of microparticles. It is anticipated that the characteristic heat storage properties of this PCM would be exhibited well in new heat storage composites.

Table 2. SEM micrographs of BCPCMs: W70C30 and W70C20PE10

The results presented in Fig. 1 show the FTIR-ATR spectra of the used virgin compounds and the BCPCM materials in the presence and absence of coffee grounds waste. Beeswax (W100) represents a complex organic mixture of many compounds, mainly analyses signals belonging to hydrocarbons, esters and free fatty acids. The main spectral bands specific to beeswax are observed in the region of the fingerprints' characteristic of the vibrations of esters and free fatty acids (at 1,739, 1,714 and 1,172 cm^{-1}). Furthermore, the absorption peaks at 2,916-2,848 cm^{-1} are characteristic of the aliphatic CH stretching vibration, the two peaks at 1,462 cm^{-1} correspond to the CH bending vibration and the two peaks at 720-730 cm^{-1} relating to the rocking vibration in the plane of the group

CH_2 . The presence of two well-resolved bands at 720 cm^{-1} and in the 1,470 cm^{-1} region in all BCPCMs spectra confirms the absence of the destruction of the long hydrocarbon components of the wax chain during the materials elaboration phase [47]. On the spectra of all blends samples without coffee grounds waste, no change in the position of the peaks and no new peaks were generated. This suggests that since there is no chemical interaction between the LDPE and beeswax, the Beeswax/LDPE blends (W/PE) at different composition were physical blends.

The FTIR spectrum obtained from coffee grounds is shown on the C100 spectrum in Fig. 1. The broad band at about 3,460 cm^{-1} included many vibrational modes mainly attributed to OH groups.

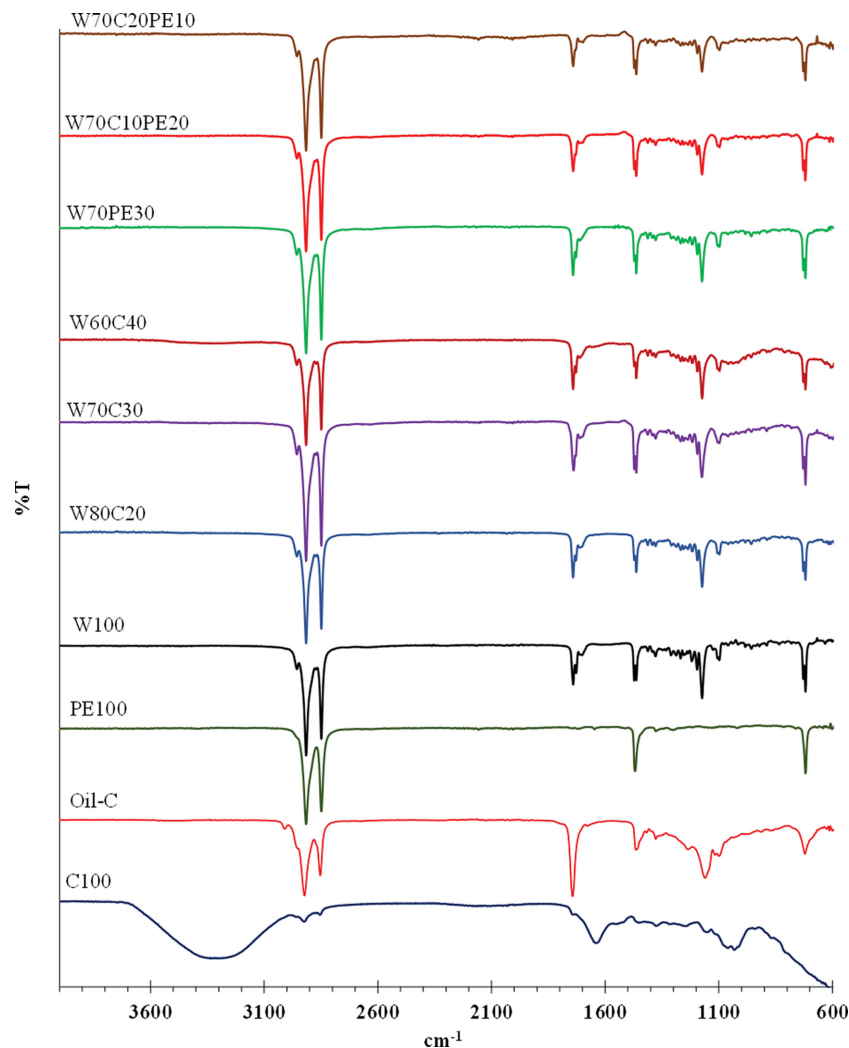


Fig. 1. FTIR spectra of virgin compounds and BCPCMs.

The presence of methyl and methylene groups is confirmed by the two sharp peaks at $2,926\text{ cm}^{-1}$ and $2,859\text{ cm}^{-1}$ attributed to asymmetric and symmetric stretching of C-H bonds in the aliphatic chains [48]. Compared with the Oil-C spectrum, the low intensity band at $1,743\text{ cm}^{-1}$ is associated with the carbonyl vibration (C=O) in the aliphatic esters or in the triglycerides of the oily fraction present in coffee grounds waste. The band at $1,640\text{ cm}^{-1}$ emanates from the C=C vibration of lipids and O-H bonds of lignocellulosic groups [49]. The band at $1,458\text{ cm}^{-1}$ corresponds to the C-H bending of the CH_3 groups. The bands observed on the spectrum of coffee grounds at $1,100\text{ cm}^{-1}$ zone are attributed to the vibrations of the C-O-C groups of the oily compounds and those of the cellulosic chains. This wide band is shown on the spectra of the composites in the presence of coffee grounds with a large % (W60C40). The exploitation of the spectral zone characteristic of the vibrations of C=O groups for samples in the presence and in the absence of micro-particles of the spent coffee grounds are shown in Fig. 2. The band around $1,740\text{ cm}^{-1}$ of the spectrum of composites containing coffee grounds, such as W70C30 and W70C20PE10, have undergone a slight shift towards the low wavenumbers. Coffee grounds-contain-

ing composites, including W70C30 and W70C20PE10, have a minor shift towards the low wavenumbers in the spectrum band around $1,740\text{ cm}^{-1}$. This displacement is linked to the formation of hydrogen bonds (C=O...HO) between the carbonyl groups of the beeswax esters and the hydroxyl functions of the cellulose in the spent coffee grounds. On the other hand, the increase in the intensity of the band at $1,741\text{ cm}^{-1}$ compared to that at $1,715\text{ cm}^{-1}$ is linked to the presence of C=O ester groups of the oily phase (in the order of 12%) in the spent coffee grounds [50]. In fact, after an extraction with hexane the oily fraction of the coffee grounds waste employed in this study exhibits a vibration band typical of the C=O groups departing at roughly $1,743\text{ cm}^{-1}$ (Fig. 2) [51].

A thermal stability index, examined by TGA measurements, is needed to determine complex BCPCM applications. Fig. 3(a) depicts the TGA curves for the W/PE blend samples. Temperatures at 10% mass loss temperature ($T_d, 10\%$) were used to describe the thermal stabilities of the samples. The TGA curves of the W/PE blends reveal a decrease in the onset of PE decomposition temperatures with the increase in wax content. The decomposition of beeswax begins at a much lower temperature than that of PE, with a differ-

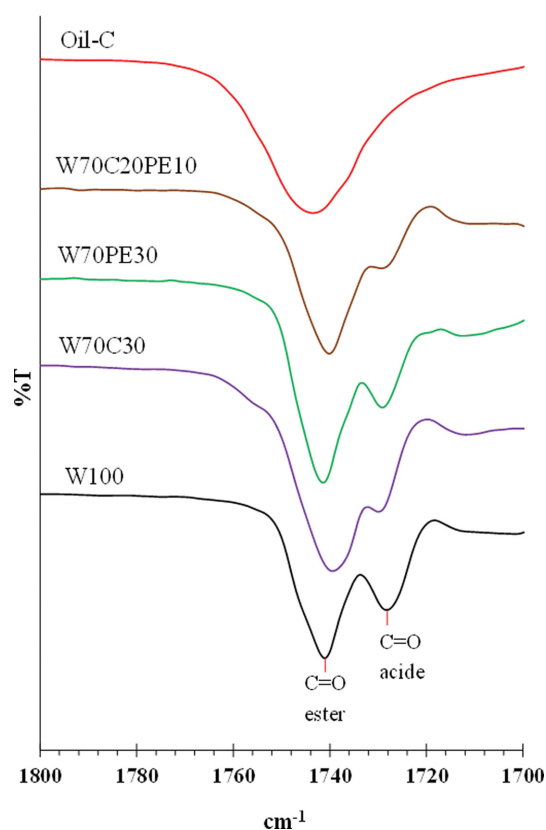


Fig. 2. Typical evolution of the C=O peak of FTIR spectra of virgin compounds and BCPCMs.

ence of nearly 200 °C between temperatures. One possible reason for the low resistance of W/PE blends to thermal degradation is the low molecular weight of the wax [52]. The TGA curves of the W/PE materials show that the thermal stability between that of pure wax and pure PE. The beeswax TGA curve indicates that the sample lost weight from about 203 °C and then changed its slope around 10% by weight from around the temperature 402 °C, characterizing the long chain molecules. While PE decomposes completely in one step, W/PE materials exhibit two-step degradation. There is a sizable difference between the decomposition temperature of pure PE and that of the W/PE blends in terms of temperatures at 10% mass loss (Td, 10%). Below 200 °C, the decomposition of the W/PE mixtures is negligible, indicating an excellent thermal stability of the mixture.

The DTG curves (Fig. 3(b)) of the blends indicate that the number of peaks corresponds to the number of degradation steps and the peak temperature corresponds to the temperature at which the maximum degradation occurs. The reason for this change is to easily convert the deflection point to a peak. The existence of two peaks indicative of the breakdown of LDPE and beeswax in the mixtures confirms their two-phase composition according to the DTG curves. The decomposition peak of beeswax was shifted towards high temperatures by the presence of LDPE. On the other hand, the temperature relative to the DTG peak of the degradation of LDPE remains constant at 473 °C. The TGA/DTG results show that all W/PE blends are degraded between 200 and 480 °C.

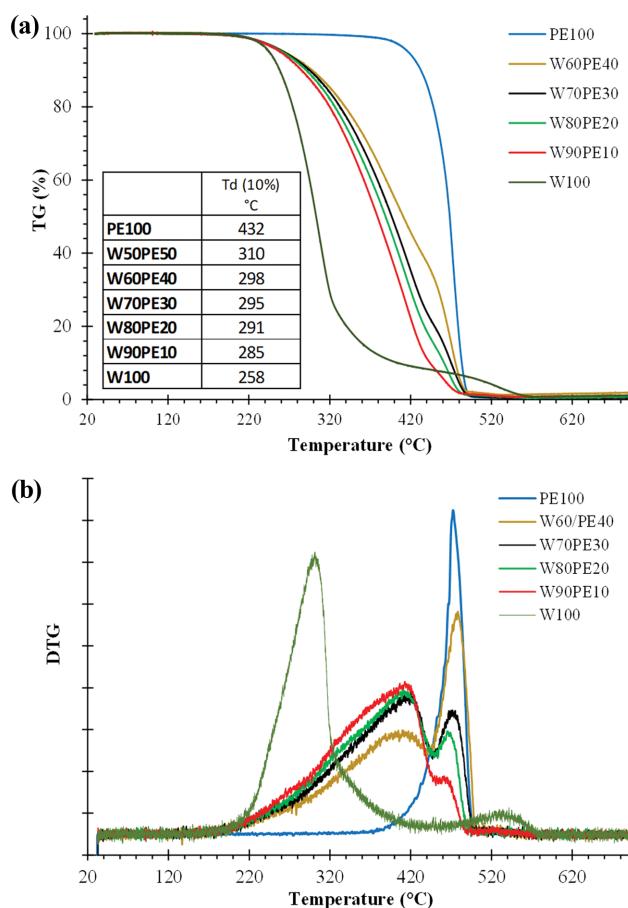


Fig. 3. TGA (a) and DTG (b) curves of LDPE, beeswax and PCM blends with different composition.

Therefore, they are expected to be stable up to 200 °C and considered to be suitably applicable to buildings.

TGA/DTG analysis was used to determine how the inclusion of coffee grounds waste affected the thermal stability of beeswax-based composites (Fig. 4). The TGA thermogram of the spent coffee ground reveals a temperature decrease of about 100 °C corresponding to the amount of water absorbed from the air's humidity [53]. The decomposition is similar to the pyrolysis properties of hemicellulose and cellulose which constitute the major components of coffee grounds. Extremely successive losses are observed on the TGA/DTG curves characteristic of hemicellulose, cellulose and other organic fraction present in coffee grounds waste [53]. In terms of the thermal stability of composites, the TGA thermogram in the presence of used coffee grounds demonstrates that these microparticles can function similarly to PE. In fact, a dramatic shift in the degradation peak on the DTG curves compared to beeswax was seen for a composition of 70% beeswax and 30% coffee grounds. The results of the TGA analyses confirm that spent coffee grounds shift the degradation temperature range of beeswax towards high temperatures. As a result, microparticles made from spent coffee grounds microparticles can therefore be used as a flame retardant in BCPCMs composites [54].

All the thermograms of the W/C/PE composites are superimposable in the temperature range from the beginning to the end of

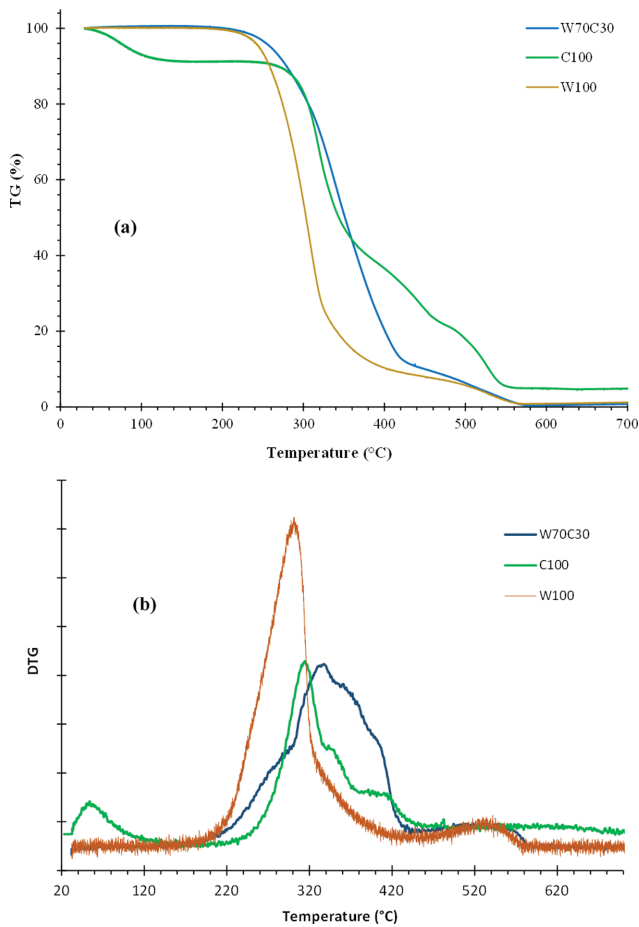


Fig. 4. TGA (a) and DTG (b) curves of beeswax and W70/C30 PCM composite.

decomposition, thus indicating a similar thermal stability (Fig. 5). It was supposed that the flammability of most compounds (derived from fats and oils) commonly used as phase change materials would

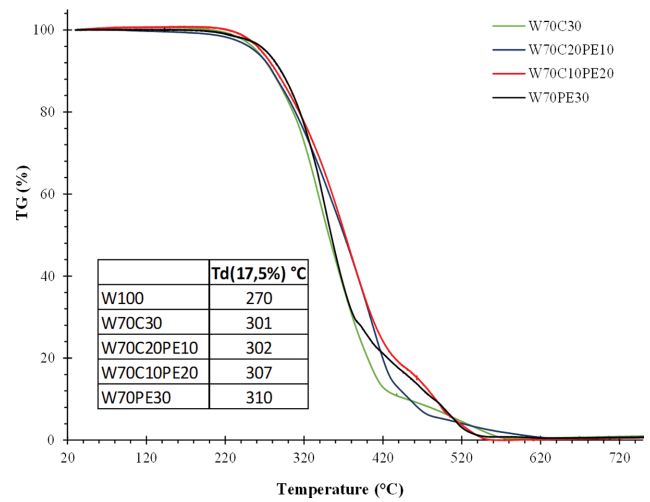


Fig. 5. TGA curves BCPCMs materials.

be directly related to the flash point of the material. To be more specific, it is assumed that the material with the lowest flash point would burn more easily. According to earlier research, TGA can be used for the determination of the flash point of oily compounds by the relative loss at 17.5% [55]. The table shows that all composites have more FPs than virgin beeswax. Hence, these composites constitute good PCMs with good thermal stability. Other than these thermal characteristics, the leakage capacity of these materials was tested as function of temperature.

1. The Shape Stability of Bio-composites

Shape stability is another crucial challenge for the practical application of organic PCMs. The experiment was performed by placing the composite with initial mass M_0 on a layer of filter paper in an oven at 60 °C. After 1 h, the sample was taken out and weighted using an analytical balance after cooling down to room temperature with the filter paper replaced following each weighing. M_n presents the mass of the sample after heating in the oven for n times.

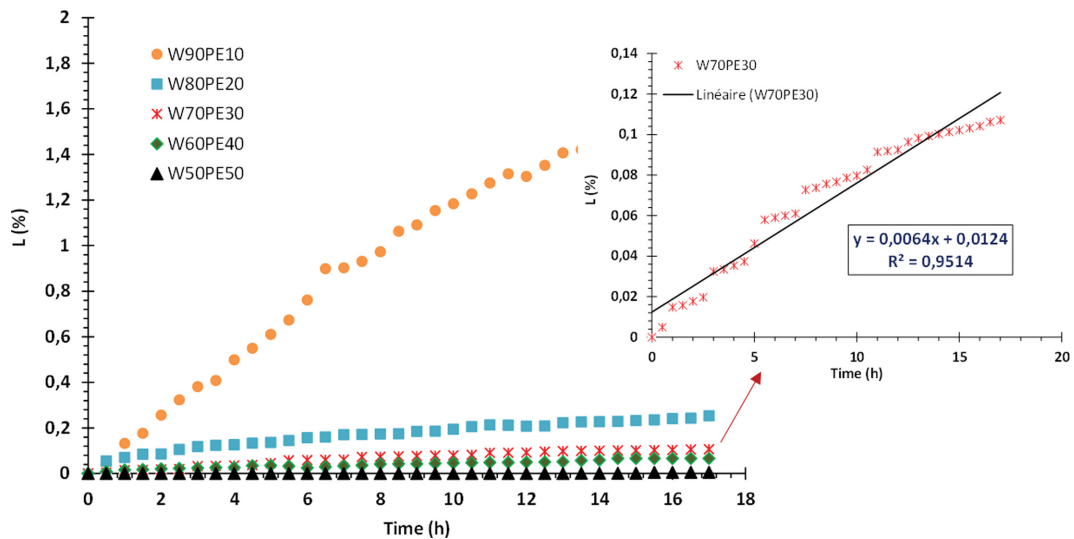
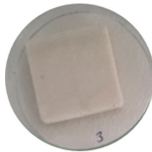
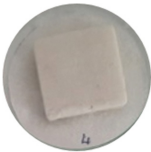


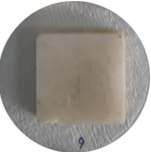







Fig. 6. Leakage tests of blends W/PE samples according to time.

Table 3. Shape-stable photographs of W/PE samples before and after thermal cycling experiment at 60 °C for 17 h

	PE10C90	PE20C80	PE30C70	PE40C60	PE50C50
Before heating					
After heating (60 °C)					

The variations of leakage L (%) as a function of time were plotted in Fig. 6 using the Eq. (1) [9]:

$$L (\%) = \frac{M_0 - M_n}{M_0} * 100 \quad (1)$$

Table 3 shows the photographs of the samples W/PE before and after being heated at 60 °C for different durations. As can be seen from Table 3, there are some imprints appear around W90/PE10 after thermal treatment. The relationships between the leakage rates and time of the composites W/PE are presented in Fig. 6. Due to residual melting on the sample surfaces, the leakage rates of the composite W/PE increased dramatically throughout the course of the 17 hour thermal cycling. The variation of the L (%) as a function of time for the composite W70/PE30 can be expressed by a fitting linear Eq. (2):

$$L (\%) = 0.0124 + 0.00646t \quad (R^2 = 0.9514) \quad (2)$$

As revealed in the equation above, at least 100 cycles are required to lose 0.6 wt% of Beeswax. This leakage test result proves that the as-prepared composite with 30% PE has an exceptional ability to keep hexadecane leakage. After 17 hours, the total leakage rates of W50PE50~W90PE10 reached 0.04%, 0.06%, 0.1%, 0.18% and 1.8%.

The relationships between the leakage rates and time of five BCPCMs (W/C and W/C/PE) are plotted in Fig. 7. The latter also demonstrates the seepage photos of all the samples on the filter paper for 17 consecutive hours of heating at 60 °C. While there is some visible leakage for the paraffins W60/C40, W70/C30, and W80/C20, there is significant leakage for the paraffins W70/C10/PE20 and W70/C20/PE10. This suggests that PE is an efficient matrix reinforcement for the melted paraffin when the mass proportion of paraffin is equal to 70%, thus enhancing the stability of the W/C BCPCMs. When PE reinforcement was added to the W/C, the sample's form stabilization effect improved (Table 4). This should be mainly attributed to the strong capillary force and intermolecular hydrogen bonding interactions between Beeswax and C/PE in the composite PCMs. The beeswax molecules were tied to the surface of C/PE by the confinement effect of strong intermolecular hydrogen bonding and lost their freedom of motion.

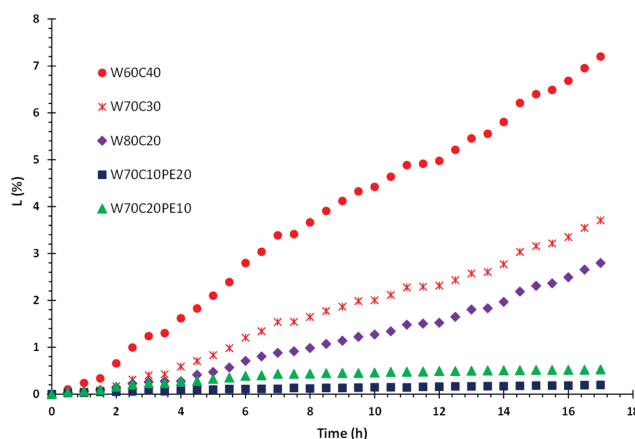


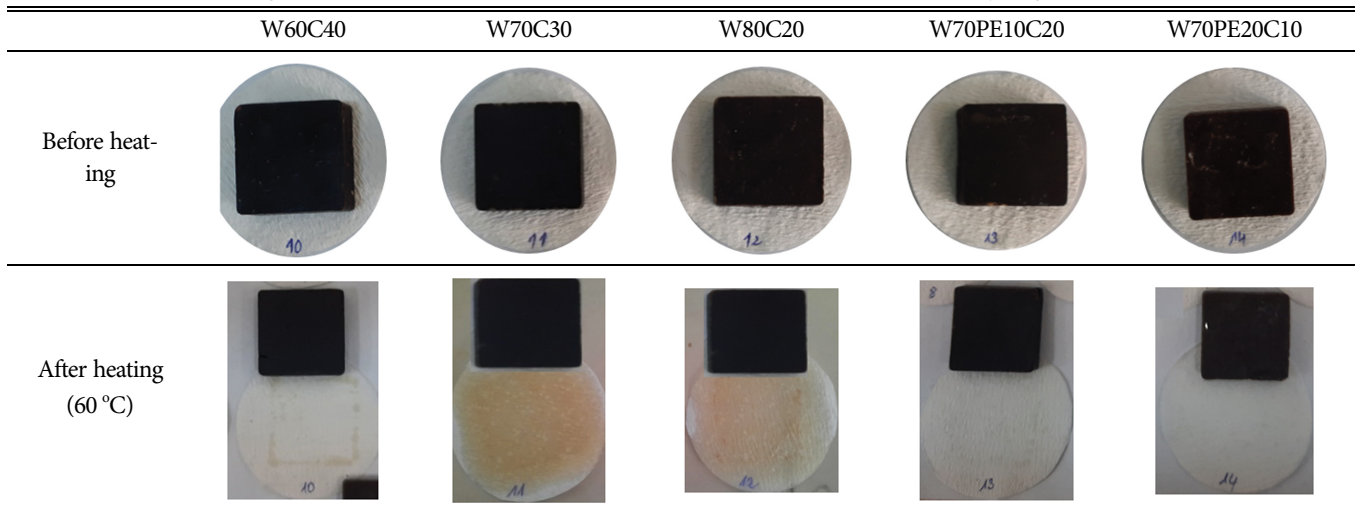
Fig. 7. Leakage tests of BCPCMs (W/C and W/C/PE) samples according to time.

The test was conducted at a temperature well over the melting point, and the findings show that no significant beeswax leakage occurred. This means that the support (C/PE) is capable of absorbing and maintaining the significant amount of liquid beeswax, producing thermally stable PCMs.

2. TES Performance of Bio-composites

DSC is an effective method to characterize the thermal behavior of PCMs, and to determine their TES capacities, in terms of transition temperature and latent heat. Using the data measured by the DSC method, it is also possible to represent the enthalpy change versus temperature and determine the amount of stored/released energy in a given temperature interval. As shown in Fig. 9, DSC thermograms illustrate the endothermic and exothermic curves for pure beeswax and pure PE, W/PE with various beeswax mass fractions, W/C-based beeswax loaded with coffee grounds, and W70C20PE10 and W70C10PE20. Table 5 provides a summary of the thermal properties that were measured.

In Fig. 8(a), the measured of the melting peak temperature ($T_{p,m}$) and solidification peak temperature ($T_{p,s}$) of the pure beeswax are 50.54 °C and 33.69 °C, respectively. The second peak at the temperature 108.68 °C in the thermograms is related to the pure PE,

Table 4. Shape-stable photographs of BCPCMs (W/C and W/C/PE) samples before and after thermal cycling experiment at 60 °C for 17 h**Table 5. Thermal properties of pure beeswax, pure PE and bio-composites**

Sample	Onset (°C)		Peak (°C)		Endset (°C)		Supercooling $\Delta T = T_{pm} - T_{ps}$
	T_{om}	T_{os}	T_{pm}	T_{ps}	T_{em}	T_{es}	
PE100	92.51	94.5	108.68	89.2	112.73	80.43	-
W100	36.41	55.09	50.54	33.69	60.28	21.29	16.82
W90PE10	32.55	56.16	50.62	34.91	63.08	18.21	15.71
W80PE20	33.23	54	50.17	34.91	58.62	27.26	15.18
W70PE30	32.62	57.58	49.43	34.91	66.26	24.9	14.53
W60PE40	33.49	57.84	50.52	34.91	66.85	23	15.61
W50PE50	37.59	58.97	51.21	34.54	68.04	25.47	16.67
W60C40	31.57	54.25	50.96	34.22	60.24	25.6	15.91
W70C30	36.78	54.51	50.06	34.22	54.43	28.42	15.56
W80C20	37.39	55.71	49.37	34.97	54.29	28.75	15.68
W70C20PE10	36.01	51.68	50.51	34.69	56.87	26.09	15.82
W70C10PE20	40.68	57.42	50.1	34.23	53.78	25.55	15.87

T_{om} : Onset melting temperature of DSC curve.

T_{os} : Onset solidification temperature of DSC curve.

T_{pm} : Melting peak temperature of DSC curve.

T_{ps} : Solidification peak temperature of DSC curve.

T_{em} : Endset melting temperature of DSC curve.

T_{es} : Endset solidification temperature of DSC curve.

whereby the Polyethylene's solidification is seen in the temperature peak 89.2 °C. In all plots, as expected, the melting points were influenced by the additives of beeswax as presented in Table 5.

After the porous material (C) was introduced, the T_{om} of the beeswax (40.68 °C, 36.01 °C, 37.39 °C, 36.78 °C, 31.57 °C for W70C10PE20, W70C20PE10, W80C20, W70C30, W60C40), as well as their T_{os} slightly decreased (57.42 °C, 51.68 °C, 55.71 °C, 54.51 °C, 54.25 °C for W70C10PE20, W70C20PE10, W80C20, W70C30, W60C40). In the blends (W/PE), the melting temperature of polyethylene decreased significantly as the wax content increased, indicating a wax plasticizing effect on LDPE. The ability of polyethylene to crystallize decreases due to the presence of miscible amorphous polymers, which leads to a decrease in melting point. On the other hand, when mixed with LDPE, the wax melting peak shows a

broadening on the higher temperature side of the peak confirming the possibility of having had some co-crystallization of the low molecular weight fractions of LDPE with wax [19]. However, there was little change in the peak melting and crystallization temperature of beeswax.

The determination of the enthalpy of BCPCM as a function of temperature with sufficient accuracy in enthalpy and temperature is an important factor representing the phase properties and crucial in PCM application. As demonstrated in Fig. 9, pure beeswax, pure PE, and bio-composites' melting (H_m) and solidification (H_s) enthalpies are compared. The measured values of ΔH_m and ΔH_s of beeswax are 175 and 169 J/g, respectively. The strong thermal heat storage capacity is reflected by a single energy endotherm of 175 J/g, which is a higher value than the heat of fusion of industrial semi-

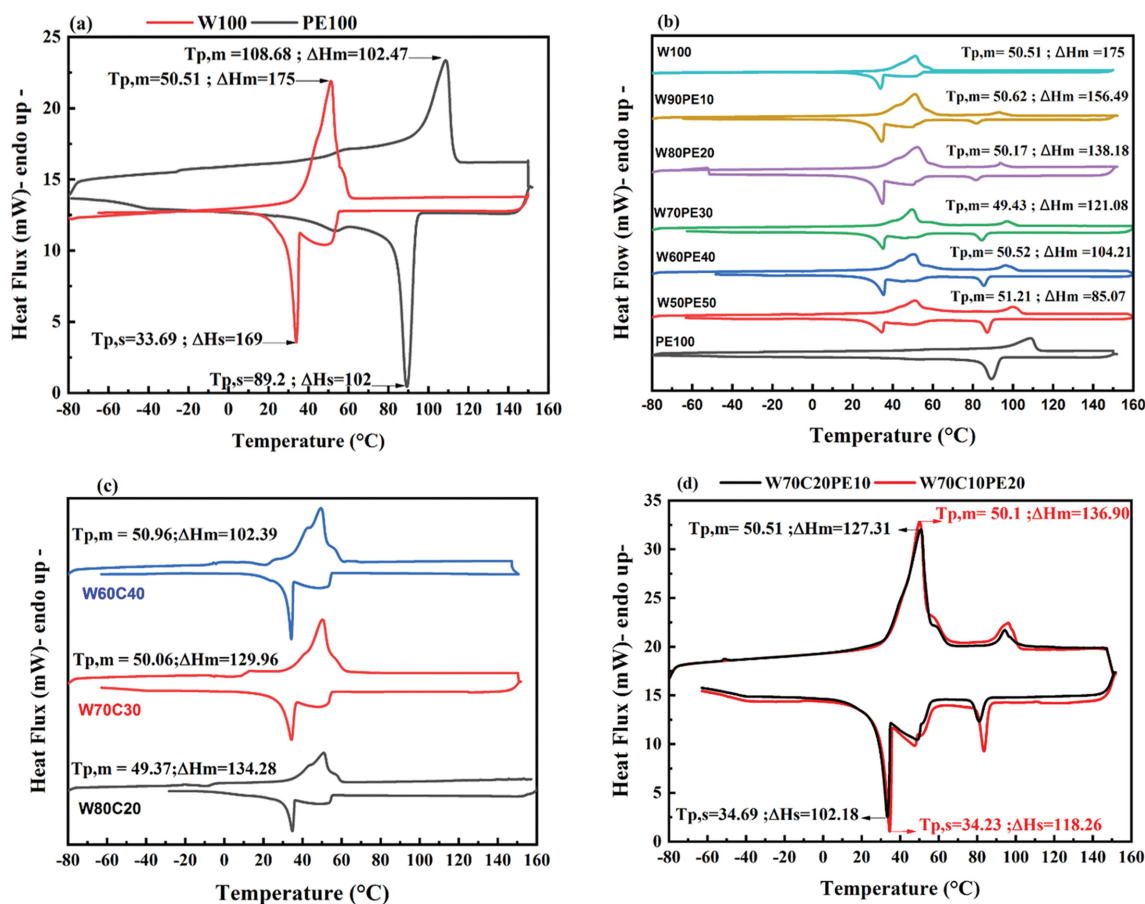


Fig. 8. DSC experiment of endothermic and exothermic thermograms for pure beeswax and PE (a) and bio-composites (b), (c) and (d).

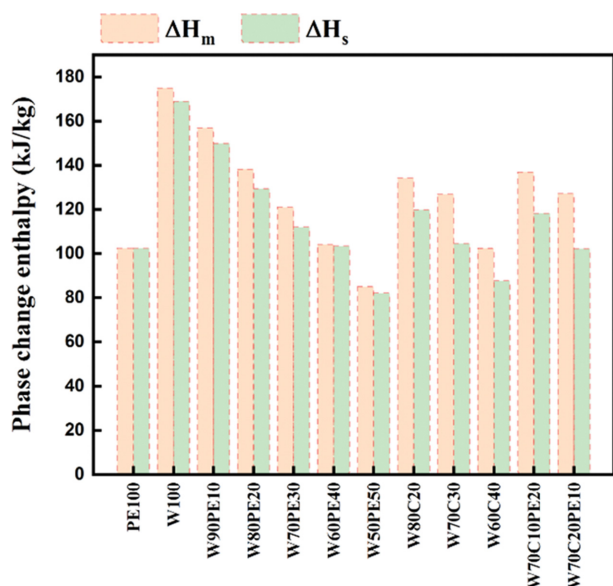


Fig. 9. Phase change enthalpies of bio-composites, pure PE and pure beeswax (PCM).

crystalline polymers such as polyesters. However, it occurs at much lower temperatures, which is ideal for phase change material application [56]. It is clear that the bio-composite latent heat increased

significantly after loading with various mass fractions of beeswax. The latent heat of W50PE50, W60PE40, W70PE30, W80PE20, W90PE10, during the heating, was 85.07 J/g, 104.21 J/g, 121.08 J/g, 138.18 J/g and 156.94 J/g, respectively. Another phase change occurs, during the cooling, and their latent heats are 82.17 J/g, 103.46 J/g, 112.05 J/g, 129.36 J/g and 149.89 J/g, respectively. The order of ΔH_m is W100 (175 J/g) > W70C10PE20 (136.9 J/g) > W70C20PE10 (127.31 J/g) > W70C30 (126.95 J/g) > W70PE30 (121.08 J/g). A comparative analysis reveals that W/C/PE has a better unit energy storage capacity than W/C and subsequently W/PE. It can also be found that the unit energy storage capacity of W/C/PE is higher than that of W/S and thereby W/PE. This is due to the capillary force and hydrogen bonding force of SCGs, which result in the formation a bio-composite with a higher unit density of beeswax [57,58].

Supercooling is a phenomenon in which the PCM starts to crystallize only at a temperature lower than the phase change temperature (melting point) as shown in Fig. 9. Latent heat is only released during energy recovery or discharge process. Crystallization cannot start until the temperature is below the phase change temperature. During the recovery of energy (discharge process), the effect of supercooling of the PCM affects the overall performance of the latent heat thermal energy storage. Supercooling is important to be minimized or stopped altogether because it degrades the efficiency of the thermal energy store for latent heat [59,60].

Supercooling prevents effective heat storage by delaying the start

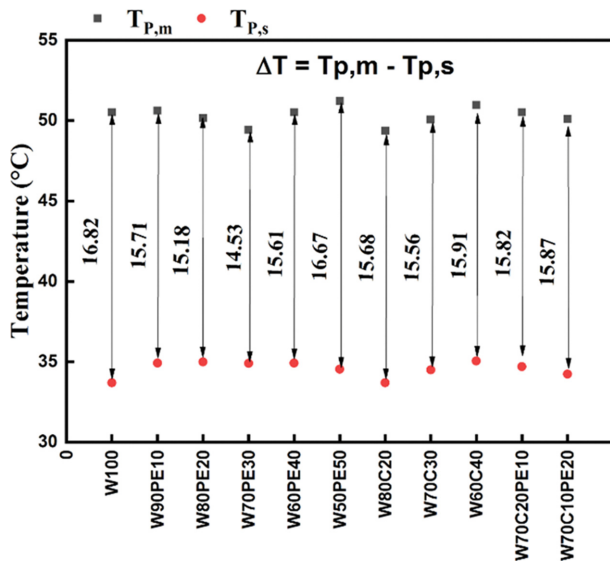


Fig. 10. Degree of supercooling of bio-composites and pure beeswax (PCM).

of solidification in phase change materials. Thus, one of the goals of creating the bio-composites is to reduce supercooling. The degree of supercooling (ΔT) of W100 and bio-composites is presented in Fig. 9. One interesting finding in Fig. 10 is that supercooling degree of all bio-composites is smaller than pure beeswax during melting/solidification process. Due to their flexible latent heat and phase-change ranges, W/C and W/C/PE composites are suited for application in thermal storage systems. Furthermore, the composites are eco-friendly and economically feasible.

3. Infrared Thermography (IRT) Analysis

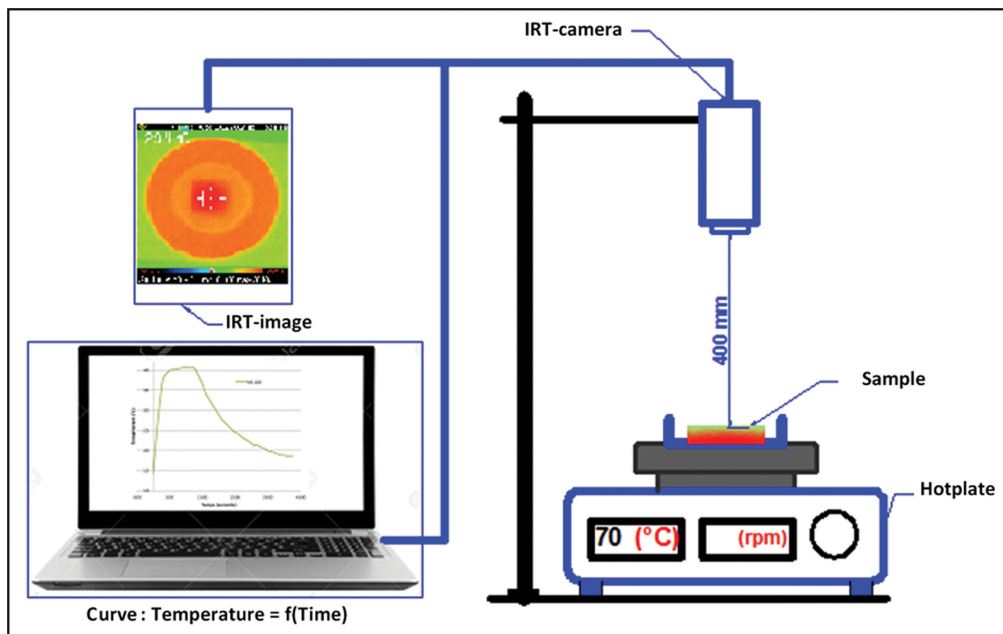
Schema 2 illustrates the schematic setups for Infrared thermography (IRT) analysis used to characterize the BCMPCs samples. A

sample of dimension 10/10 mm was placed on a glass petri dish on a hot plate. The thermal camera was placed at a distance of 400 mm to record the IR images (Schema 2).

Fig. 11 shows the surface temperature behavior images captured by an IR camera to investigate the thermal absorption-release properties of the materials. The heating -up experimentation was carried out on the samples to investigate the thermal storage capacity. As shown in the scale bar, the black, dark blue color represents the coldest, and yellow, red representing the highest temperature. The thermal scans show that an immediate and uniform hot region steadily grew from the top to the center, with the belly tip at the center [61].

According to Fig. 12, the composite W70PE30 shows faster thermal responses to charging (melting) in only 2,862 s. The sample W70C30 possesses an accumulated heat; it turned to a darker color more slowly until 4,133 s. The storage process of W70C20PE10 happened at a higher temperature and showed faster response to charging compared to the reference W100.

In comparison to the other samples, the pure spent coffee ground (C100) had a quicker thermal storage and release response. It was found each mix has a distinct point for each mix where the surface temperature starts rising more quickly, which is a point occurring when all beeswax melted. When the surface temperature exceeded the melting point of PCM, the temperature controlling the capacity of the beeswax gradually decreased. At this stage, the energy is once again accumulating in the matrix as sensible heat [62]. By comparing them with those of W100, the heat storage and release properties of the bio-composite PCMs are evaluated. The temperature response curves of samples over time were collected (Fig. 12). The heating time of W70PE30 and W70C20PE10 is shorter by 25 and 20%, respectively, than that of W100. Moreover, the composite W70C30 leads to a slower time response rate. Compared to W100, the heating time of W70C30 increased by 8.5%. After remov-



Schema 2. Schematic representation of the infrared thermography (IRT) analysis process.

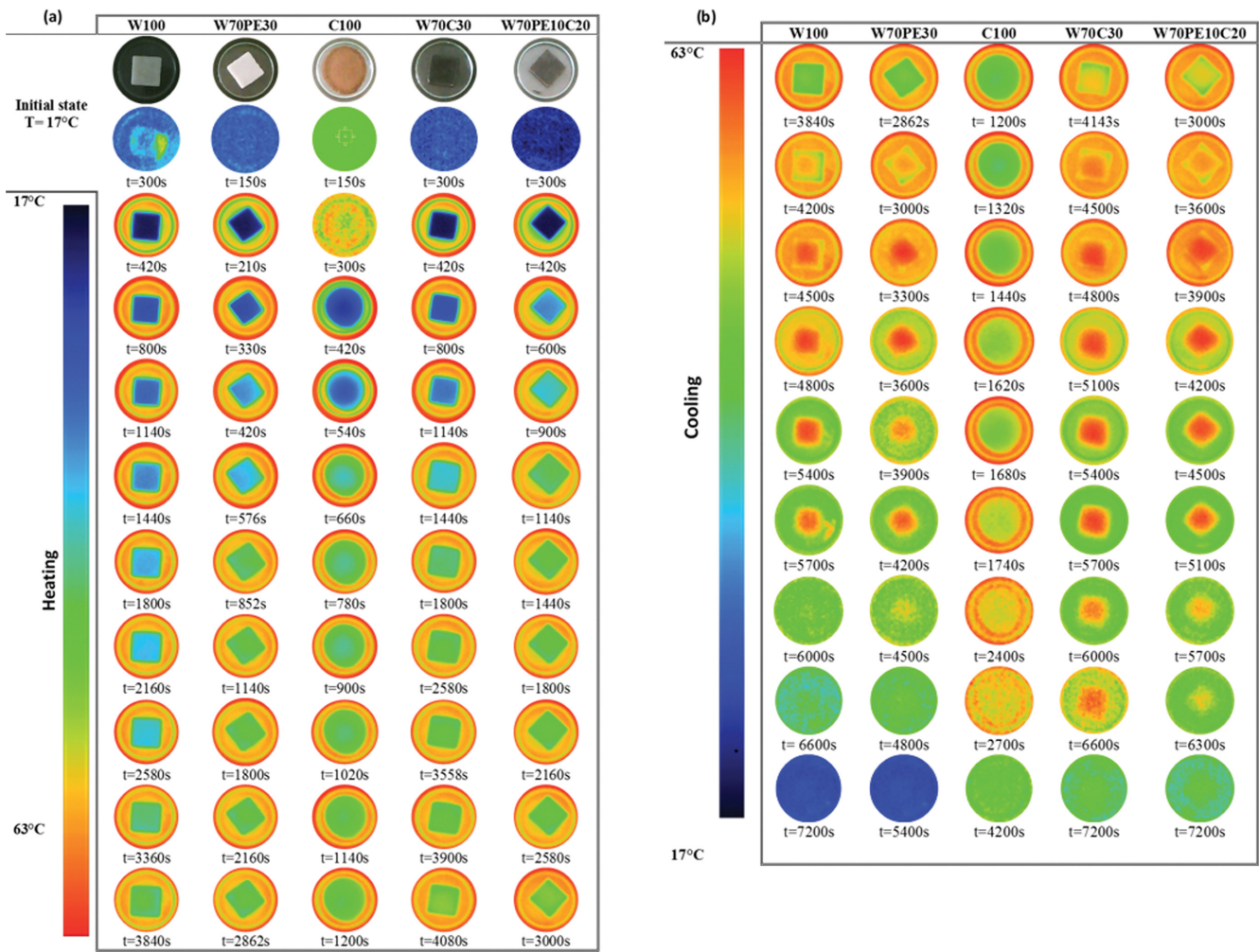


Fig. 11. Infrared thermographs of BCPCMs samples: (a) heating and (b) cooling.

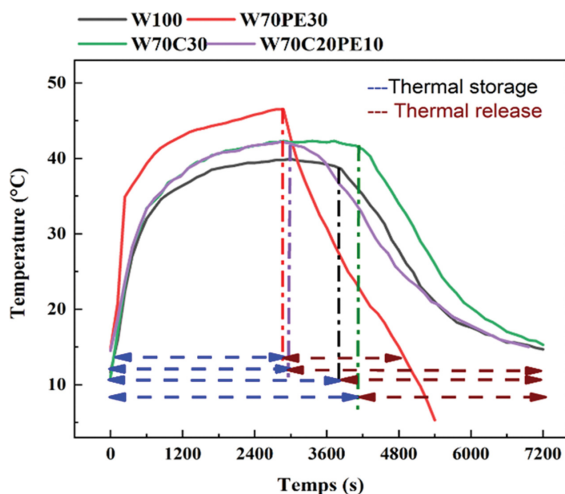


Fig. 12. Temperature curves as a function of time for pure beeswax and BCPCM samples.

ing the hot plate, the temperature of the mixture W70C30 slowly decreases from 41.4 °C to 15.45 °C within 3,047 s. The discharg-

ing times of thermal energy for the W100 is about 3,380 s. Due to the thermal insulation of the inner PCM, the surface temperatures of W70PE30 and W70C20PE10 decrease to 13.5 °C after cooling for 2,030 s and 3,326 s, respectively. In the cooling process, in contrast to the fastest decrease of the temperature of the W70PE30, the temperature of W70C30 dropped slower and become longer. By adding PE to the PCM, the melting time is reduced, demonstrating an improvement in the TES reaction time to the demand. However, when the solidification process began, the energy release process took a very long time to complete. On the upper surface of the substance that was in contact with the heated plate, a layer of solid PCM developed, which is attributed to the development of a microscopic layer that “insulates” the liquid PCM from the source of cooling [63]. Moreover, it can be noted that the period of solidification was much longer than the melting process.

CONCLUSION

Innovative latent heat storage biocomposites (LHSBCs) were prepared using LDPE, spent coffee grounds and Beeswax as bio-PCMs. These bio-PCMs are inexpensive blends with a good physical and

chemical stability. The SEM images and FT-IR results proved that Beeswax was successfully loaded and evenly dispersed in the porous network of coffee grounds particles without any chemical reaction between them. The prepared BCPCMs exhibited excellent shape and stability even when the temperature was much higher than the melting point of Beeswax, and it is due to the good structure for incorporating liquefied materials. DSC analysis results indicated that blends containing coffee grounds microparticles exhibit better unit energy storage capacity. The extent of supercooling of all bio-composites is less than pure beeswax during melting/solidification process. Due to the addition of spent coffee grounds, CBPCMs shift the degradation temperature range of beeswax towards high temperatures at 365 °C. As a result, spent coffee grounds microparticles can be used as a flame retardant in BCPCMs composites. Infrared thermography analysis showed the storage process of bio-composite W70C20PE10 occurred at a higher temperature than W70PE30 and W70C30 with a faster response to charging compared to the PCM reference W100. So that, we can conclude that compositions with W70C20PE10 are interesting for industrial purposes as they are environmentally friendly BCPCMs and can be considered as a promising PCM materials for environmental benefits, due to good shape stability, heat capacity satisfactory latent temperature and excellent thermal stability.

REFERENCES

1. A. Korjenic, J. Zach and J. Hroudová, *Energy Build.*, **116**, 45 (2016).
2. A. Putra, K. H. Or, M. Z. Selamat, M. J. M. Nor, M. H. Hassan and I. Prasetiyo, *Appl. Acoust.*, **136**, 9 (2018).
3. S. K. Karmee, *Waste Manag.*, **72**, 240 (2018).
4. A. Trigui, M. Karkri, C. Boudaya, Y. Candau and L. Ibos, *Compos. Part B Eng.*, **49**, 22 (2013).
5. C. Moulahi, A. Trigui, C. Boudaya and M. Karkri, *J. Therm. Compos. Mater.*, **30** (2017).
6. S. H. Lee, S. J. Yoon, Y. G. Kim, Y. C. Choi, J. H. Kim and J. G. Lee, *Korean J. Chem. Eng.*, **24**, 332 (2007).
7. G. Alva, Y. Lin, L. Liu and G. Fang, *Energy Build.*, **144**, 276 (2017).
8. C. Moulahi, A. Trigui, M. Karkri and C. Boudaya, *Compos. Struct.*, **149**, 69 (2016).
9. I. Chriaa, A. Trigui, M. Karkri, I. Jedidi, M. Abdelmouleh and C. Boudaya, *Appl. Therm. Eng.*, **171**, 115072 (2020).
10. F. Xue, X. Jin, W. Wang, X. Qi, J. Yanga and Y. Wang, *Nanoscale*, **12**, 4005 (2020).
11. F. Asinger, *Paraffins; chemistry and technology*, Pergamon Press. (1967).
12. A. I. de Barros, F. H. Nunes and M. a Costa, Manual de boas práticas na produção de cera de abelha, 1 (2009).
13. A. Sharma, V. V. Tyagi, C. R. Chen and D. Buddhi, *Renew. Sustain. Energy Rev.*, **13**, 318 (2009).
14. V. Saydam and X. Duan, *J. Therm. Anal. Calorim.*, **135**, 1135 (2019).
15. J. A. Baptista and M. E. S. Eusébio and M. M. Pereira, *J. Therm. Anal. Calorim.*, **145**, 27 (2021).
16. Y. Hong and G. Xin-shi, *Sol. Energy Mater. Sol. Cells.*, **64**, 37 (2000).
17. H. Inaba and P. Tu, *Heat Mass Transf.*, **32**, 307 (1997).
18. A. Trigui, M. Karkri and I. Krupa, *Energy Convers. Manag.*, **77**, 586 (2014).
19. I. Krupa, G. Miková and A. S. Luyt, *Eur. Polym. J.*, **43**, 4695 (2007).
20. A. Jering, J. Günther, A. Raschka and M. Carus, *ETC/SCP Rep.*, 1 (2010).
21. M. Maleki, A. Imani, R. Ahmadi, H. Banna Motejadded Emrooz and A. Beitollahi, *Appl. Energy*, **258**, 114108 (2020).
22. R. Campos-Vega, G. Loarca-Piña, H. A. Vergara-Castañeda and B. Dave Oomah, *Trends Food Sci. Technol.*, **45**, 24 (2015).
23. S. I. Mussatto, E. M. S. Machado, S. Martins and J. A. Teixeira, *Food Bioprocess Technol.*, **4**, 661 (2011).
24. S. Kim, S. J. Chang, O. Chung, S.-G. Jeong and S. Kim, *Energy Build.*, **70**, 472 (2014).
25. D. García-García, A. Carbonell, M. D. Samper, D. García-Sanoguera and R. Balart, *Compos. Part B Eng.*, **78**, 256 (2015).
26. O. Das, D. Bhattacharyya, D. Hui and K.-T. Lau, *Compos. Part B Eng.*, **106**, 120 (2016).
27. S. Calligaris, M. Munari, G. Arrighetti and L. Barba, *Lipid Sci. Technol.*, **111**, 1270 (2009).
28. C. S. Wu, *Polym. Degrad. Stab.*, **121**, 51 (2015).
29. L. F. Ballesteros, M. A. Cerqueira, J. A. Teixeira and S. I. Mussatto, *Carbohydr. Polym.*, **127**, 347 (2015).
30. G. M. A. Khan, M. S. A. Shams, M. R. Kabir, M. A. Gafur, M. Terano and M. S. Alam, *Appl. Polym. Sci.*, **128**, 1020 (2013).
31. N. Saba, M. Jawaid, O. Y. Allothman and M. T. Paridah, *Constr. Build. Mater.*, **106**, 149 (2016).
32. T. Väisänen, O. Das and L. Tomppo, *J. Clean. Prod.*, **149**, 582 (2017).
33. J. Yoo, S. J. Chang, S. Wi and S. Kim, *Chemosphere*, **235**, 626 (2019).
34. E. Pagalan, M. Sebron, S. Gomez, S. J. Salva, R. Ampusta, A. J. Macarayo, C. Joyno, A. Ido and R. Arazo, *Ind. Crops Prod.*, **145**, 111953 (2020).
35. X. Hu, H. Huang, Y. Hu, X. Lu and Y. Qin, *Sol. Energy Mater. Sol. Cells*, **219**, 110790 (2021).
36. M. Rinaudo, *Prog. Polym. Sci.*, **31**, 603 (2006).
37. A. El Kadib and M. Bousmina, *Chem. A Eur. J.*, **18**, 8264 (2012).
38. P. Hao, Z. Zhao, Y. Leng, J. Tian, Y. Sang, R. I. Boughton, C. P. Wong, H. Liu and B. Yang, *Nano Energy*, **15**, 9 (2015).
39. R. M. Obaidat, B. M. Tashtoush, M. F. Bayan, R. T. Al Bustami and M. Alnaief, *AAPS PharmSciTech*, **16**, 1235 (2015).
40. R. Yu, Y. Shi, D. Yang, Y. Liu, J. Qu and Z.-Z. Yu, *ACS Appl. Mater. Interfaces*, **9**, 21809 (2017).
41. S. Takeshita and S. Yoda, *Chem. Mater.*, **27**, 7569 (2015).
42. A. El Kadib, *ChemSusChem*, **8**, 217 (2015).
43. L. Boussaba, A. Foufa, S. Makhlof, G. Lefebvre and L. Royon, *Constr. Build. Mater.*, **185**, 156 (2018).
44. H. Essabir, M. Raji, S. A. Laaziz, D. Rodrique, R. Bouhfid and A. el kacem Qaiss, *Compos. Part B Eng.*, **149**, 1 (2018).
45. I. Krupa, Z. Nógellová, Z. Špitalský, M. Malíková, P. Sobolčák, H. W. Abdelrazeq, M. Ouederni, M. Karkri, I. Janigová and M. A. S. A. Al-Maadeed, *Thermochim. Acta*, **614**, 218 (2015).
46. M. A. Al Maadeed, S. Labidi, I. Krupa and M. Ouederni, *Arab. J. Chem.*, **8**, 388 (2015).
47. V. Y. Birshtein and V. M. Tulchinskii, *Chem. Nat. Compd.*, **13**, 232 (1977).
48. I. B. Perry, T. F. Brewer, P. J. Sarver, D. M. Schultz, D. A. DiRocco and D. W. C. MacMillan, *Nature*, **560**, 70 (2018).
49. M. A. Abdalla, *Int. J. Eng. Appl. Sci.*, **2**, 85 (2015).
50. D. J. Lyman, R. Benck, S. Dell, S. Merle and J. Murray-Wijelath, *J.*

- Agric. Food Chem.*, **51**, 3268 (2003).
51. A. E. Atabani, S. Shobana, M. N. Mohammed, G. Uğuz, G. Kumar, S. Arvindnarayan, M. Aslam and A. H. Al-Muhtaseb, *Fuel*, **244**, 419 (2019).
52. A. Bucio, R. Moreno-Tovar, L. Bucio, J. Espinosa-Dávila, F. Anguebes-Franceschi, *Coatings*, **11**, 261 (2021).
53. L. F. Ballesteros, J. A. Teixeira and S. I. Mussatto, *Food Bioprocess Technol.*, **7**, 3493 (2014).
54. H. Vahabi, M. Jouyandeh, T. Parpaite, M. R. Saeb and S. Ramakrishna, *Coatings*, **11**, 1021 (2021).
55. A. Abdelkhalik, H. Elsayed, M. Hassan, M. Nour, A. B. Shehata and M. Helmy, *Egypt. J. Pet.*, **27**, 131 (2018).
56. A. Trigui, M. Karkri, L. Peña, C. Boudaya, Y. Candau, S. Bouffi and F. Vilaseca, *J. Compos. Mater.*, **47**, 1387 (2013).
57. T. Qian, J. Li, X. Min, Y. Deng, W. Guan and H. Ma, *Energy*, **82**, 333 (2015).
58. M. H. Zahir, M. M. Rahman, K. Irshad, M. M. Rahman, *Nanomaterials*, **9**, 1773 (2019).
59. I. Chriaa, M. Karkri, A. Trigui, I. Jedidi, M. Abdelmouleh and C. Boudaya, *Polymer*, **212**, 123128 (2021).
60. G. R. Solomon, S. Karthikeyan and R. Velraj, *Appl. Therm. Eng.*, **52**, 505 (2013).
61. A. Nejman, E. Gromadzińska, I. Kamińska and M. Cieślak, *Molecules*, **25**, 122 (2020).
62. A. Trigui, M. Karkri, C. Boudaya, Y. Candau, L. Ibos and M. Fois, *J. Compos. Mater.*, **48**, 49 (2014).
63. A. Trigui, M. Abdelmouleh and C. Boudaya, *RSC Adv.*, **12**, 21990 (2022).